

## Electronic Supporting Information (ESI)

### A new anionic metal-organic framework showing tunable emission by lanthanide(III) doping and high selective CO<sub>2</sub> adsorption properties

Rong-Ying Chen,<sup>a</sup> Dan Tian,<sup>a</sup> Yun-Wu Li,<sup>a</sup> Ying-Bin Lv,<sup>a</sup> Hong-Wei Sun,<sup>a</sup> Ze Chang\*,<sup>a</sup> and Xian-He Bu<sup>a</sup>

<sup>a</sup> Department of Chemistry, TKL of Metal- and Molecule-Based Material Chemistry, Key Laboratory of Advanced Energy Materials Chemistry (MOE), and Collaborative Innovation Center of Chemical Science and Engineering (Tianjin), Nankai University, Tianjin 300071, P. R. China.

### Contents

1. Infrared (IR) spectra;
2. Thermogravimetric analysis (TGA);
3. Additional structure figures;
4. PXRD patterns;
5. Table S1 Selected bond distances and angles;
6. Gas adsorption measurements.

\*To whom correspondence should be addressed. E-mail: [changze@nankai.edu.cn](mailto:changze@nankai.edu.cn) (Ze Chang).

**1. Infrared (IR) spectra.**

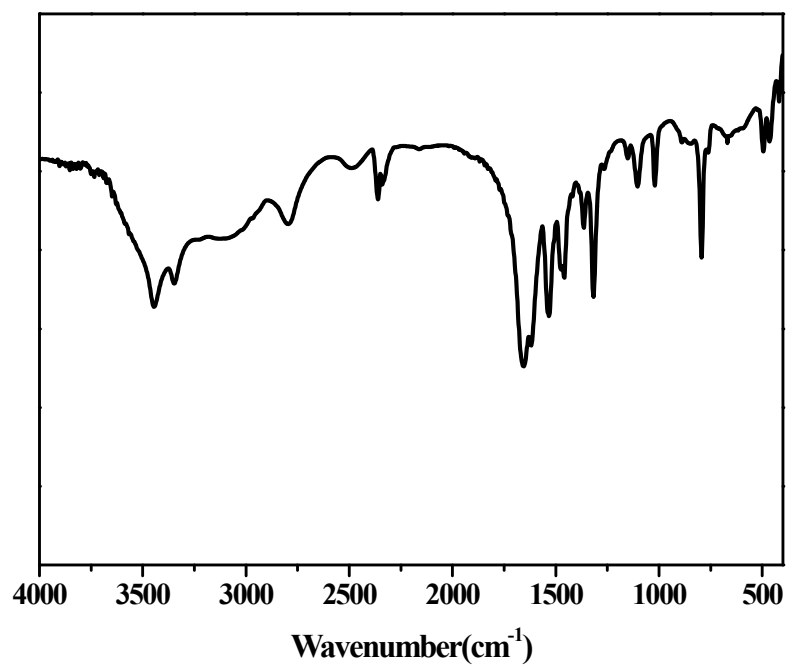


**Fig. S1** IR spectrum of **1**.

**2. Thermogravimetric analysis (TGA).**

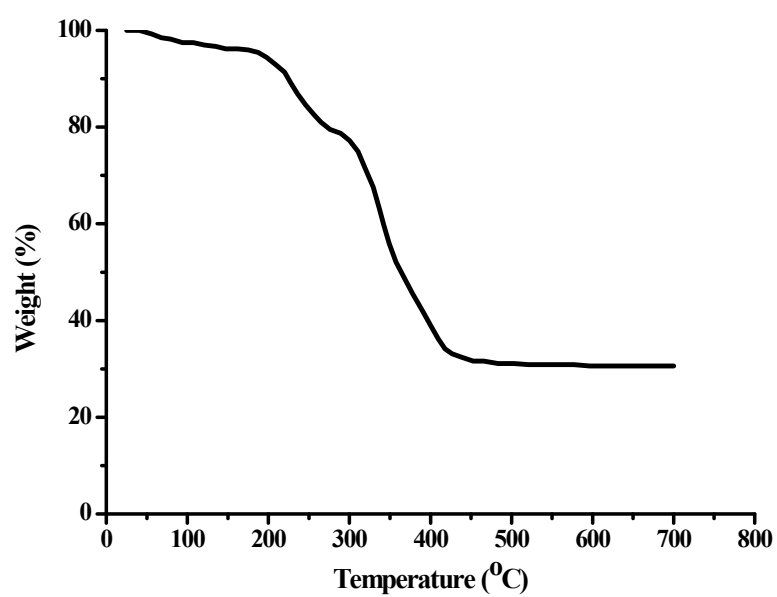


**Fig. S2** Thermogravimetric curve of **1**.

### 3. Additional structure figures.

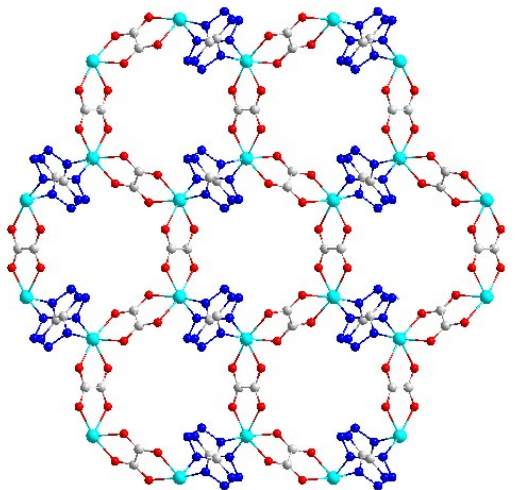


**Fig. S3** The shape of the pore along *c*-axis.

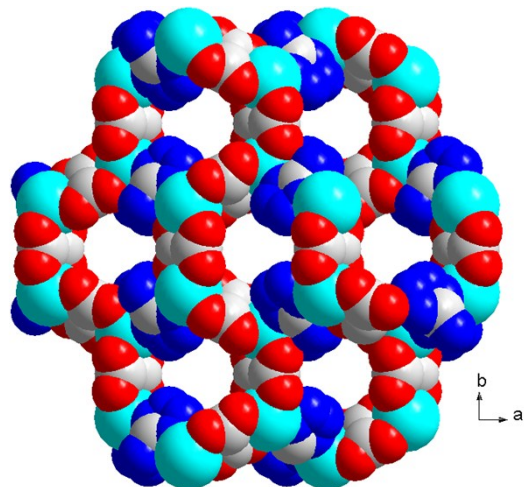


**Fig. S4** Space-filling representation of the 3D open framework along *c*-axis.

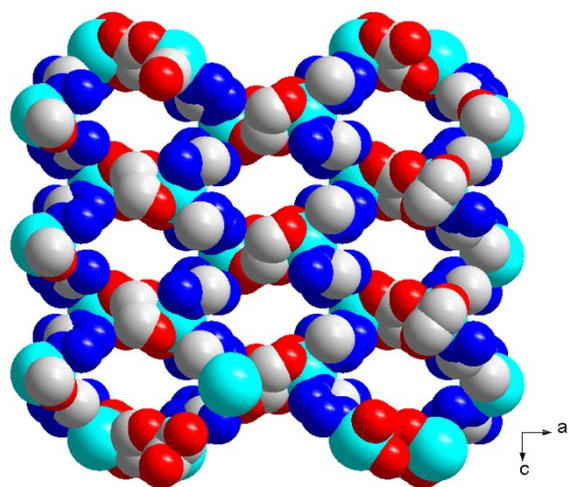


**Fig. S5** Space-filling representation of the 3D open framework along *b*-axis.

#### 4. PXRD patterns.

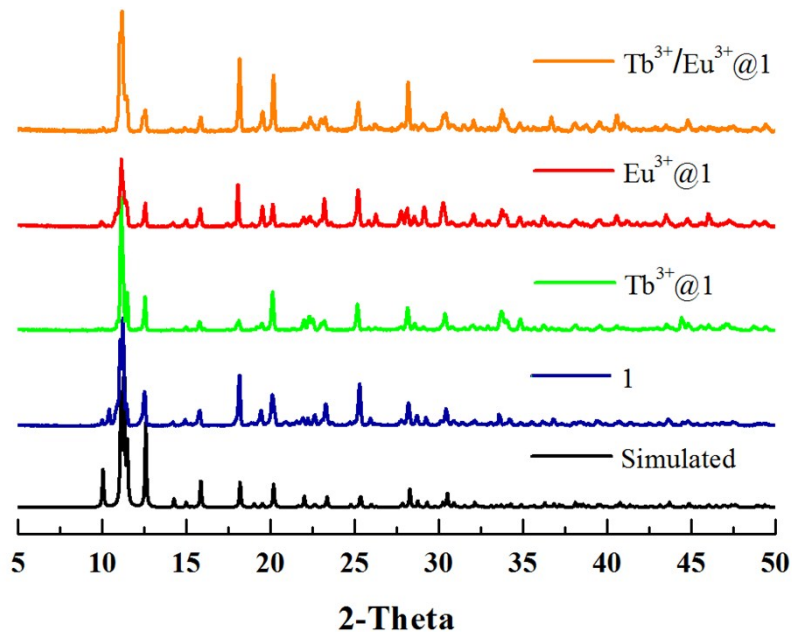


**Fig. S6** PXRD patterns of the simulated **1**, as-synthesized **1**,  $\text{Tb}^{3+}@1$ ,  $\text{Eu}^{3+}@1$  and  $\text{Tb}^{3+}/\text{Eu}^{3+}@1$  samples.

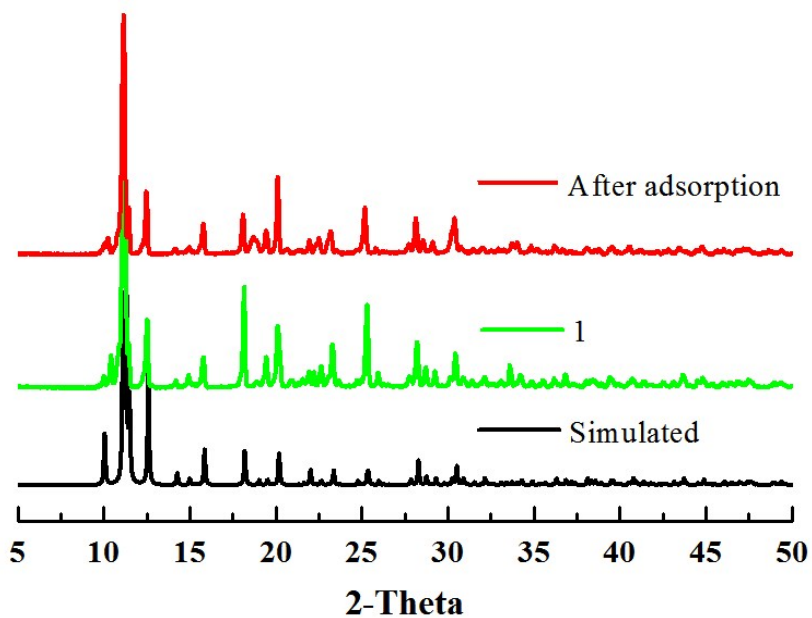


**Fig. S7** The PXRD patterns of **1**: the simulated pattern based on X-ray single-crystal data (black), the as-synthesized (green) and the pattern after gas adsorption measurements (red).

**5. Table S1 Selected bond distances and angles.**

**Table S1** Selected bond distances ( $\text{\AA}$ ) and angles ( $^\circ$ ) of **1**.

Complex <b>1</b>			
N(1)-Zn(1)	2.101(4)	N(4)-Zn(1)#3	2.103(4)
O(1)-Zn(1)	2.094(3)	O(2)-Zn(1)	2.208(3)
O(3)-Zn(1)	2.188(3)	O(4)-Zn(1)#2	2.108(3)
O(1)-Zn(1)-N(1)	100.34(14)	O(1)-Zn(1)-N(4)#4	88.32(14)
N(1)-Zn(1)-N(4)#4	94.05(15)	O(1)-Zn(1)-O(4)#2	165.49(13)
N(1)-Zn(1)-O(4)#2	91.94(13)	N(4)#4-Zn(1)-O(4)#2	98.56(14)
O(1)-Zn(1)-O(3)	90.45(12)	N(1)-Zn(1)-O(3)	168.28(13)
N(4)#4-Zn(1)-O(3)	90.81(14)	O(4)#2-Zn(1)-O(3)	76.77(12)
O(1)-Zn(1)-O(2)	77.11(12)	N(1)-Zn(1)-O(2)	90.79(14)
N(4)#4-Zn(1)-O(2)	165.26(14)	O(4)#2-Zn(1)-O(2)	95.17(12)
O(3)-Zn(1)-O(2)	87.13(13)		

Symmetry codes: #2: -x, -y, -z + 2; #4: -x + 1/2, -y, z + 1/2.

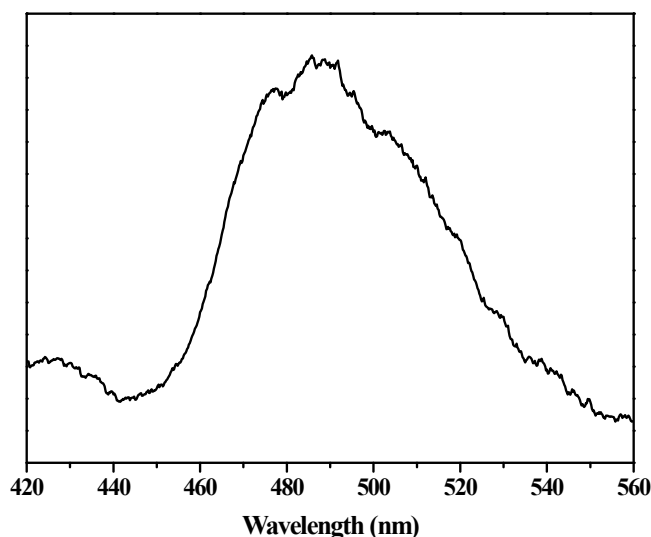


**Fig. S8** Solid-state emission spectra of Hatz.

## 6. Gas adsorption measurements.

Samples of complex **1** and **Eu<sup>3+</sup>@1** were treated with supercritical CO<sub>2</sub> in a Tousimis™ Samdri® PVT-30 critical point dryer. Prior to drying, the samples were soaked in absolute ethanol to exchange the occluded solvent for C<sub>2</sub>H<sub>5</sub>OH for 72 h. Then the ethanol-containing samples were placed inside the dryer and the ethanol was exchanged with CO<sub>2</sub> (liquid) over a period of 6 hrs according to literature.<sup>S1</sup> During this time the liquid CO<sub>2</sub> was vented under positive pressure for five minutes each hour. The processed samples were loaded in sample tubes and activated under high vacuum at 50 °C for **1**. Degassed samples were used for gas sorption measurements. Gas adsorption measurements were performed using an ASAP 2020 Surface Area and Porous analyzer.

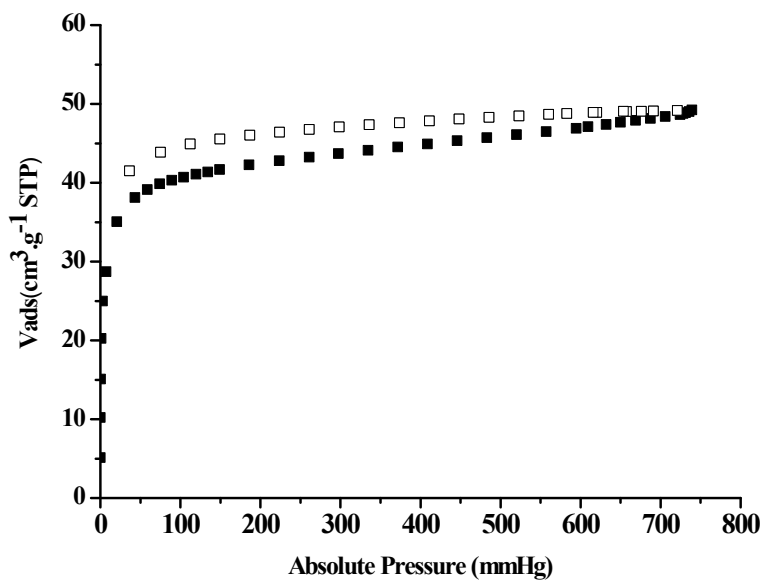


**Fig. S9** Gas adsorption isotherms of CO<sub>2</sub> in **1** at 195 K (adsorption and desorption branches are shown with closed and open symbols, respectively).

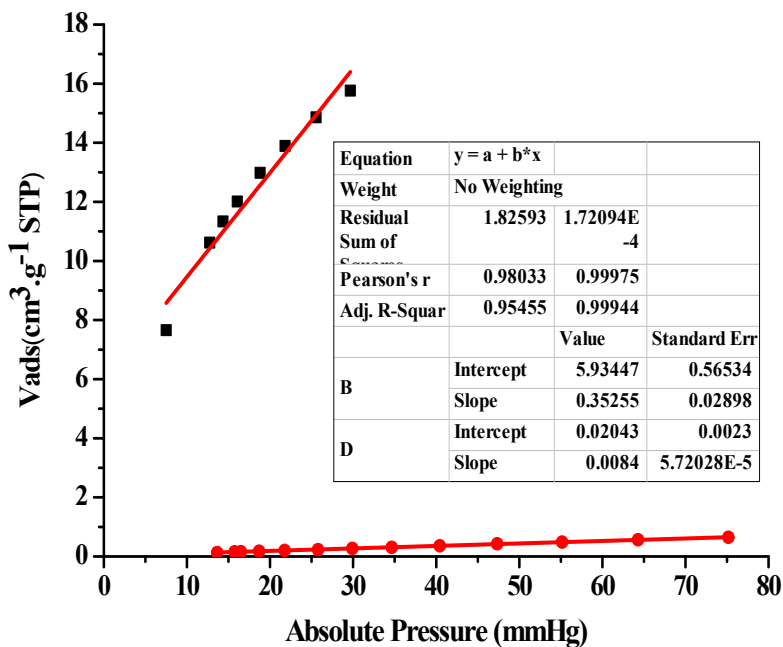


**Fig. S10** The fitting initial slopes for CO<sub>2</sub> and CH<sub>4</sub> isotherms of **1** at 273 K.

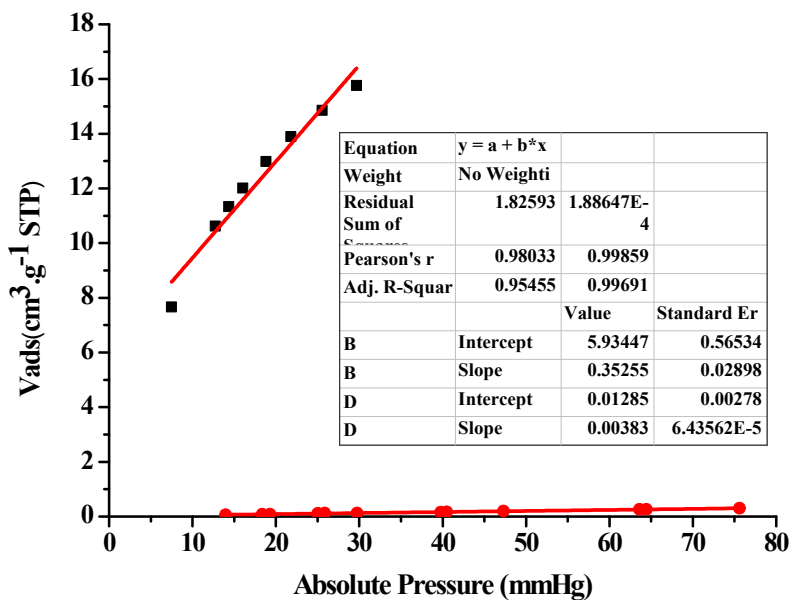


**Fig. S11** The fitting initial slopes for CO<sub>2</sub> and N<sub>2</sub> isotherms of **1** at 273 K.

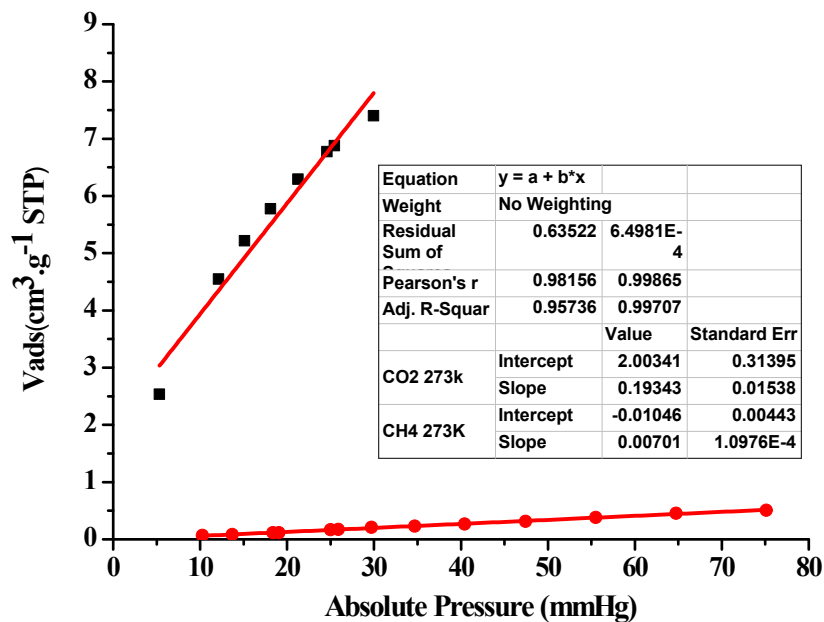


**Fig. S12** The fitting initial slopes for CO<sub>2</sub> and CH<sub>4</sub> isotherms of Eu<sup>3+</sup>@1 at 273 K.

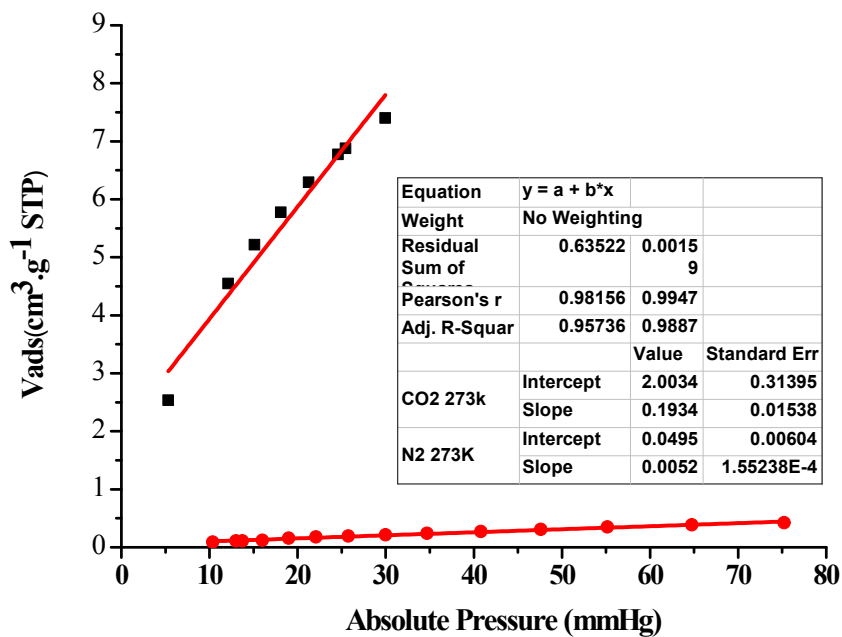


**Fig. S13** The fitting initial slopes for CO<sub>2</sub> and N<sub>2</sub> isotherms of Eu<sup>3+</sup>@1 at 273 K.

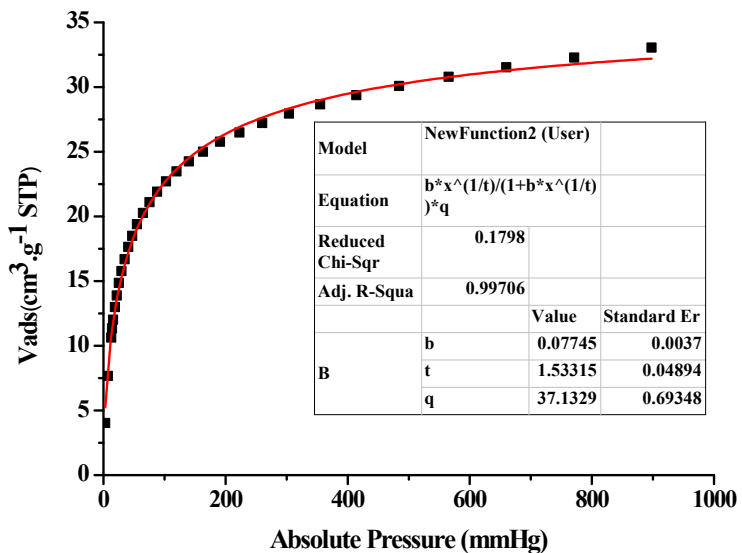


**Fig. S14** CO<sub>2</sub> adsorption isotherm for **1** fitted by the Clausius-Clapeyron equation at 273 K.

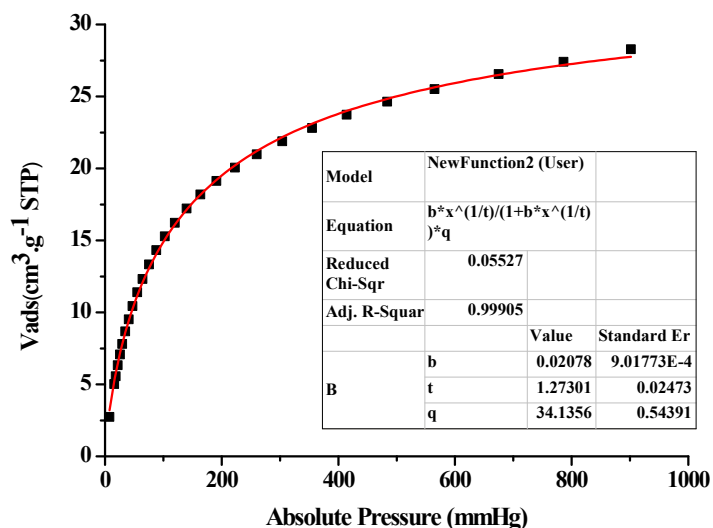


**Fig. S15** CO<sub>2</sub> adsorption isotherm for **1** fitted by the Clausius-Clapeyron equation at 298 K.

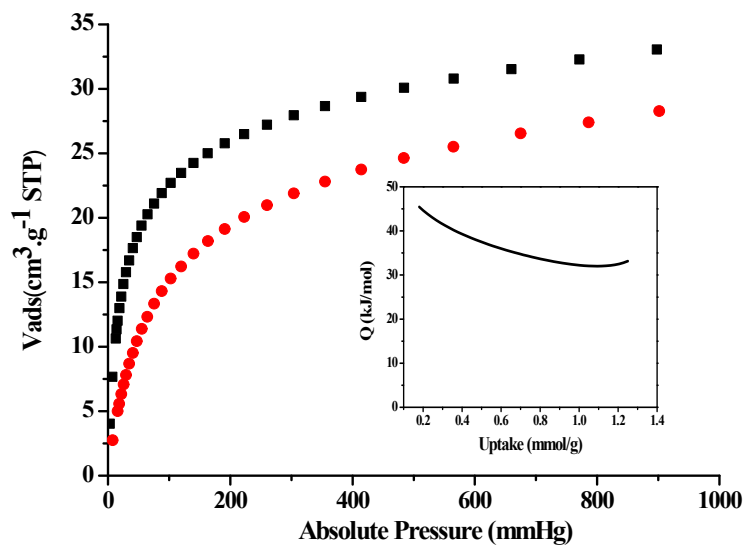


**Fig. S16** Gas adsorption isotherms of  $\text{CO}_2$  at 273 K and 298 K for **1**. Inset shows the adsorption heat ( $Q_{\text{st}}$ ) depending on gas uptake.

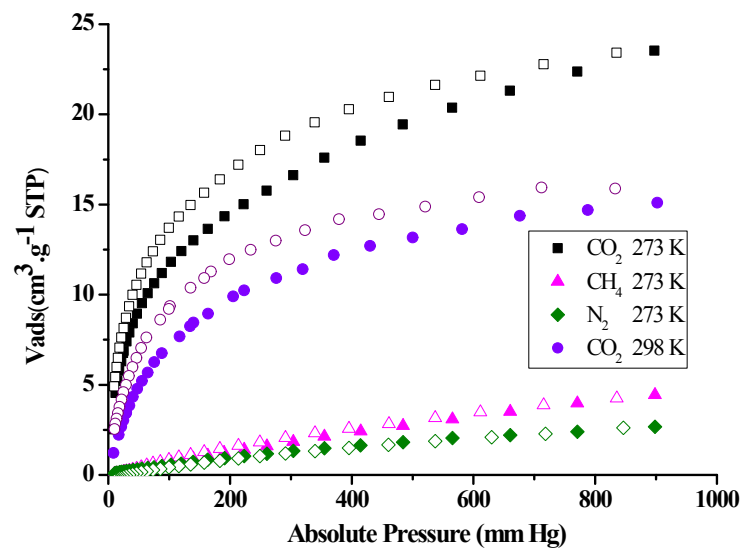


**Fig. S17** Gas adsorption isotherms of  $\text{CO}_2$ ,  $\text{CH}_4$  and  $\text{N}_2$  at 273 K and  $\text{CO}_2$  at 298 K for  $\text{Eu}^{3+}@1$ .

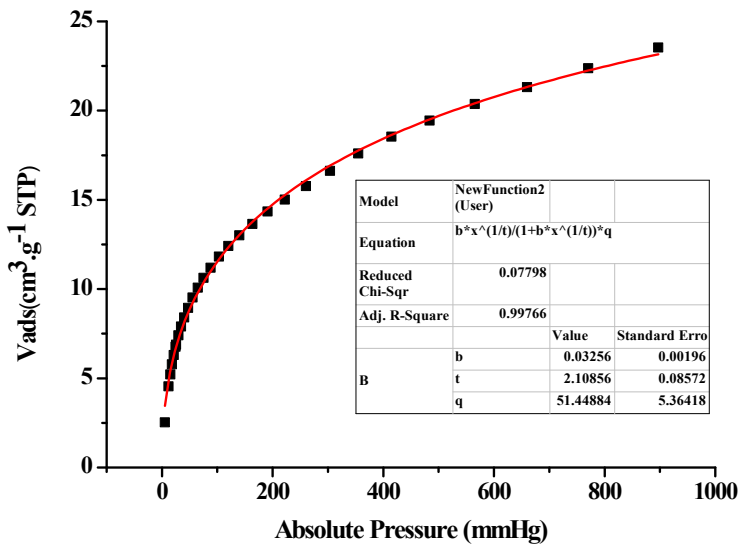


**Fig. S18** CO<sub>2</sub> adsorption isotherm for Eu<sup>3+</sup>@1 fitted by the Clausius-Clapeyron equation at 273 K.

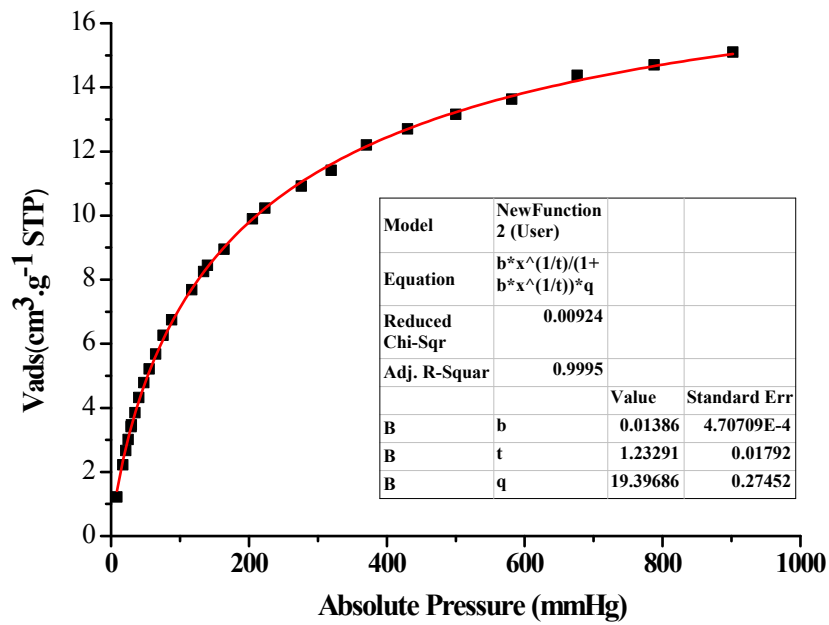


**Fig. S19** CO<sub>2</sub> adsorption isotherm for Eu<sup>3+</sup>@1 fitted by the Clausius-Clapeyron equation at 298 K.

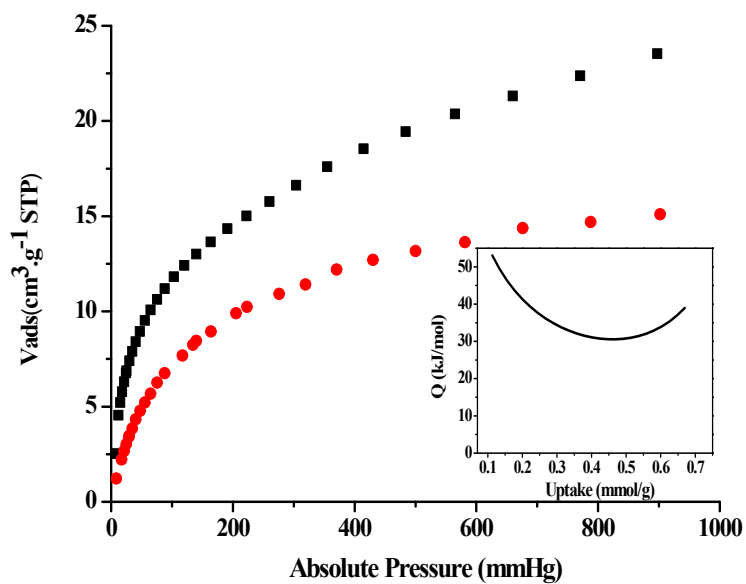


**Fig. S20** Gas adsorption isotherms of CO<sub>2</sub> at 273 K and 298 K for Eu<sup>3+</sup>@1. Inset shows the adsorption heat ( $Q_{\text{st}}$ ) depending on gas uptake.

## References.

- S1 A. P. Nelson, O. K. Farha, K. L. Mulfort, J. T. Hupp, *J. Am. Chem. Soc.*, 2009, **131**, 458.